

Physics Potential of a Photon Collider

- SM : Higgs physics \rightarrow $\left\{ \begin{array}{l} H \rightarrow \gamma\gamma \\ \text{CP properties} \end{array} \right.$

• New Physics :

\rightarrow Complementarity of e^+e^- and $\gamma\gamma$ colliders for new physics searches

\rightarrow Some specific examples :

- Anomalous G.B. couplings
- LQ's
- Composite / Excited fermions
- Extra Dim's
- NC QFT (JoAnne's talk)

T. Rizzo
6/0

If/when the Higgs boson is found, we must examine all of its properties in detail !

The SM Higgs is expected to be light

$$113 \leq m_H \lesssim 200 \text{ GeV at } 95\% \text{ CL}$$

with the possibility that $m_H \approx 115 \text{ GeV}$
(thanks Maiani !)

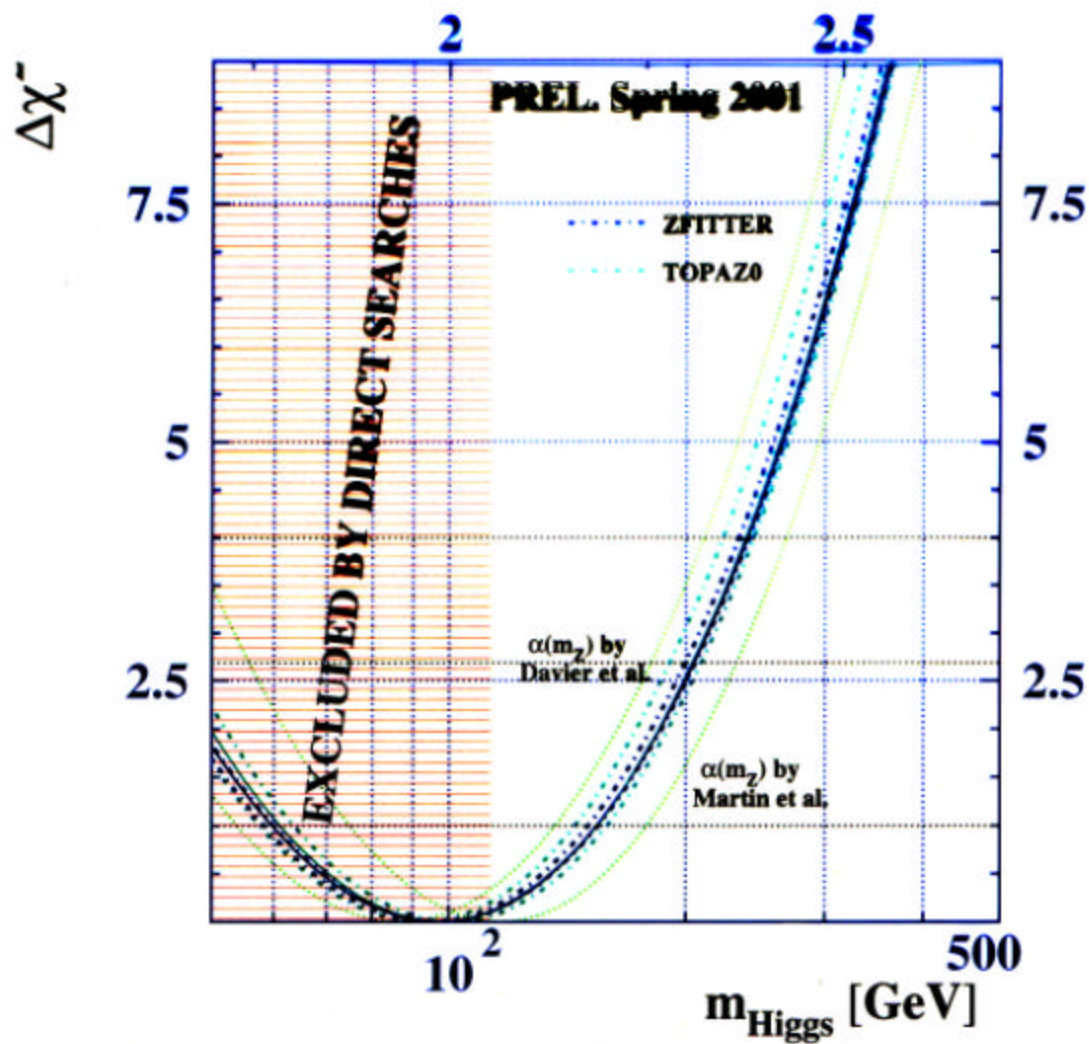
$H \rightarrow \gamma\gamma$ is a very important decay mode to understand which will be invisible at the Tevatron or any e^+e^- collider

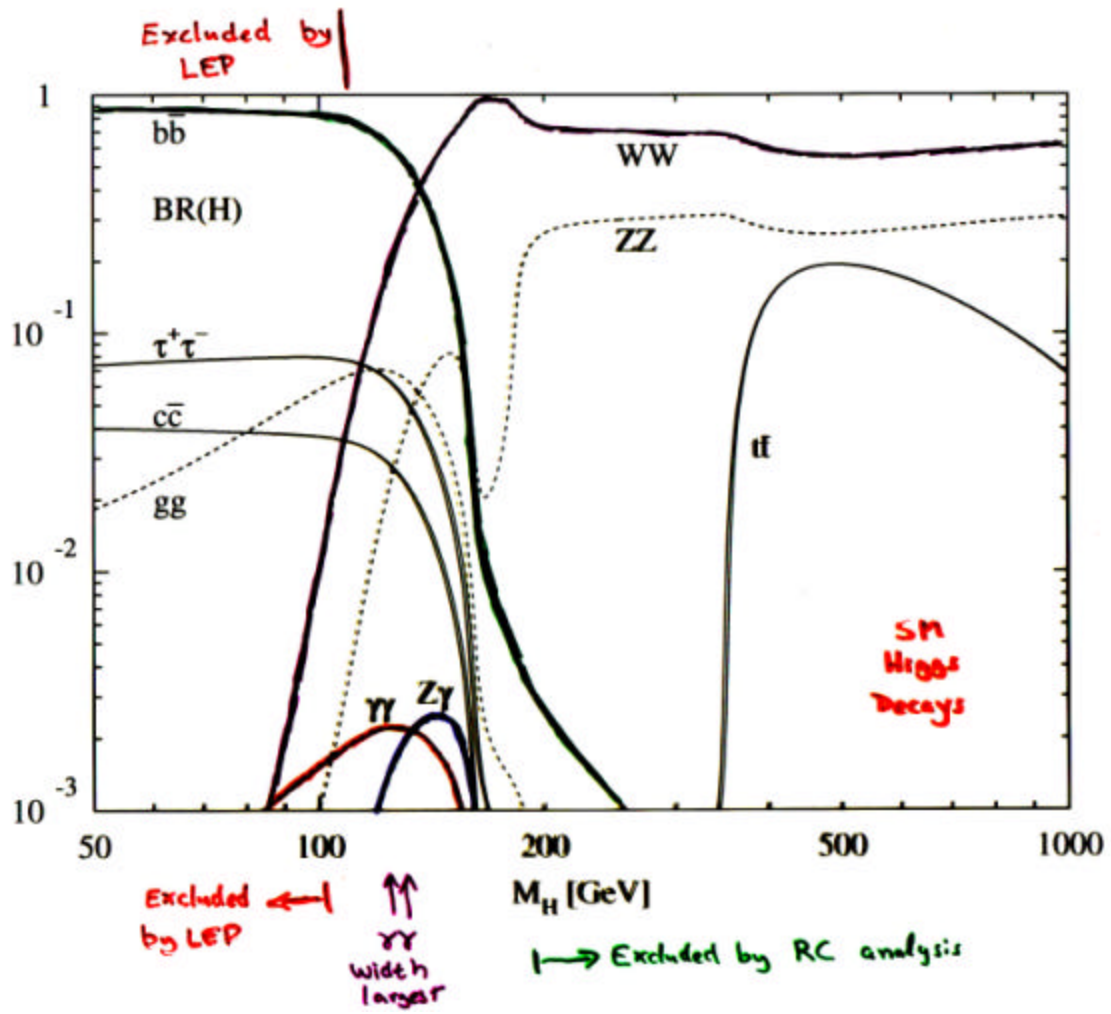
But may be the LHC discovery mode

But even then it won't be well-measured

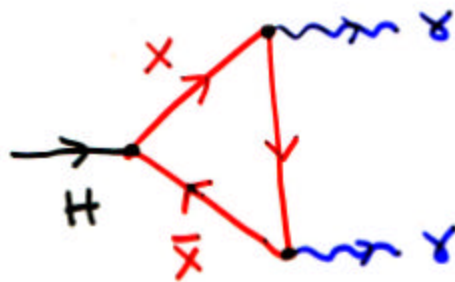
Why is this mode ... as rare as it is ... so

important ??





IT probes indirectly for any, new charged particles which couple to Higgs !!



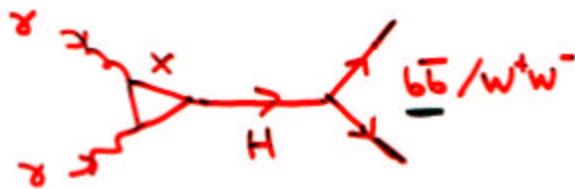
In the SM

$X = \underline{W \text{ and } t}$

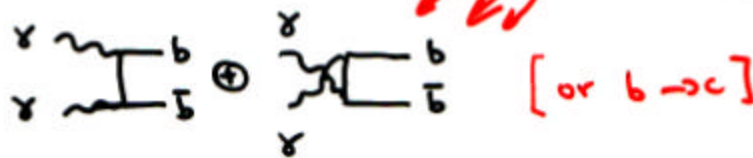
(+ b, c, s, u, d, e, μ , ...)

But it's easy to imagine all sort's of heavy stuff that can't be produced that may contribute [besides SM !!] { due to kinematics }

→ To the rescue comes the photon collider by turning the graph around



But there are more conventional backgrounds in the SM



$$\frac{d\sigma}{d\cos\theta} (\gamma\gamma \rightarrow b\bar{b}) \Big|_{J_2=0} \sim \beta(1-\beta^4) \sim \frac{m_b^2}{s}$$

Higgs channel !!

$$\frac{d\sigma}{d\cos\theta} (\gamma\gamma \rightarrow b\bar{b}) \Big|_{J_2=2} \sim \beta^3$$

Use of $\gamma\gamma$ polarization to pick out $J_2=0$ channel important

⇒ tree-level SM is suppressed in Higgs channel ($J_2=0$)

!!! But this leads to large Radiative Corrections that need to be treated carefully to quite high order
 { Melles, Stirling + Khoze[†]; Jikia; Braaten & Leveille, ...
 which are now under control for both background + signal. (to quite high order....)

- The signal is a "narrow peak" on a continuum background .. except for $b\bar{b}$ resolution effects

[†] A detailed analysis is presented by Melles, Stirling + Khoze PRD61, 054015 (2000)

Ratio of Signal to
Background
Events

Melles,
Stirling + Khoze

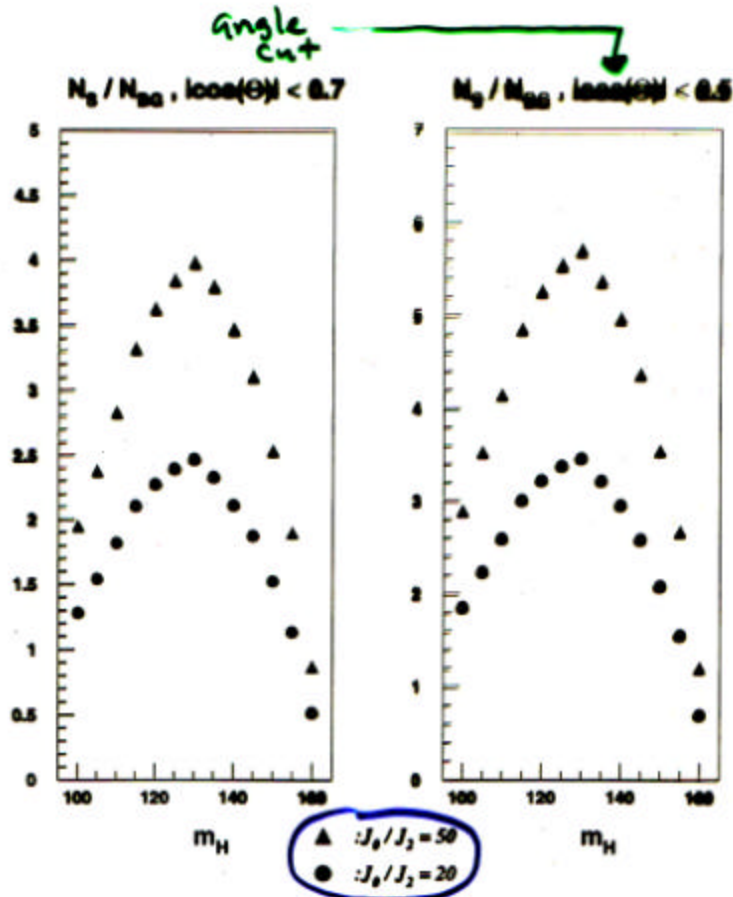


Figure 7: The ratio of signal to background events based on the jet parameters of Fig. 6. The smaller phase space cut $|\cos \theta| < 0.5$ gives a larger ratio as expected.

$$\gamma\gamma \rightarrow H \rightarrow b\bar{b}$$

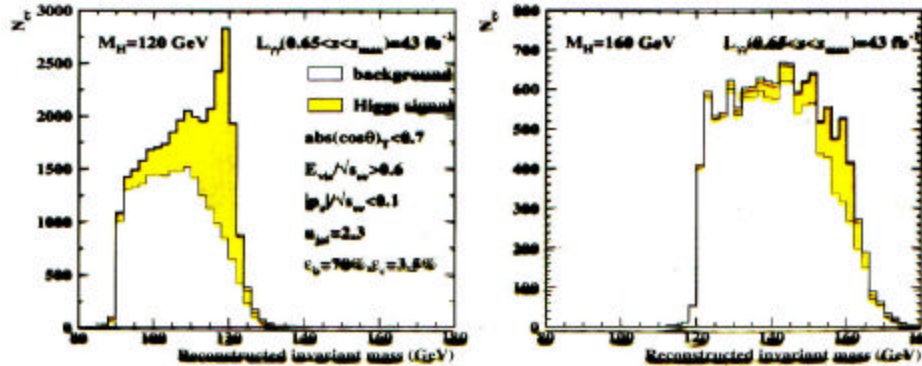


Figure 13.1: Mass distributions for the Higgs signal and heavy quark background for a Higgs mass of 120(left) and 160(right) GeV from Söldner-Rembold and Jikia [5]. The reduced signal-to-background at 160 GeV reflects the diminished branching ratio to $b\bar{b}$ near the WW threshold.

Very heavy Higgs bosons, such as those present in the MSSM, can also be produced as s -channel resonances in $\gamma\gamma$ collisions. In the MSSM, these heavy states have suppressed couplings to gauge bosons and may be most easily observed in $b\bar{b}$ or $t\bar{t}$ final states. These states may escape discovery at the LHC for intermediate values of $\tan\beta$. At e^+e^- colliders they can only be produced via associated production, $e^+e^- \rightarrow HA$, and thus lie outside the kinematic reach of the machine if their mass exceeds 240 GeV. The single production mode of the $\gamma\gamma$ collider allows the discovery reach to be extended to over 400 GeV. The $\gamma\gamma$ collider also allows one to separate degenerate H and A states and to study possible CP-violating mixing between H and A using linear polarization.

2.2 Supersymmetric particle production

For production significantly above threshold, sfermion and charged Higgs boson pairs have production cross sections in $\gamma\gamma$ collisions that are larger than those in e^+e^- annihilation. Thus, $\gamma\gamma$ collisions can provide an excellent laboratory for their detailed study. In addition, $\gamma\gamma$ production isolates the electromagnetic couplings of these particles, whereas in e^+e^- the Z and possible t -channel exchanges are also present. Thus complementary information can be obtained by combining data extracted from the two production processes. It should be noted that the search reach for new particles is typically somewhat greater in e^+e^- because of the kinematic cut-off of the photon spectra. However, the SUSY process $\gamma e \rightarrow \tilde{e}_{L,R}\chi_1^0$ shows that there are exceptions to this rule; the threshold for this process can be significantly below that for \tilde{e} pair production in e^+e^- collisions when the χ_1^0 is light. In the study of this reaction, both the \tilde{e} and χ_1^0 masses can be determined.

Given the present level of QCD/QED corrections + anticipated $\gamma\gamma$ lumi

$$\rightarrow \Delta [\Gamma_{\gamma\gamma} B_{b\bar{b}}] / \Gamma_{\gamma\gamma} B_{b\bar{b}} \approx 2\%$$

and LC $\rightarrow B_{b\bar{b}}$ to 1%

$$\rightarrow \Delta \Gamma_{\gamma\gamma} / \Gamma_{\gamma\gamma} \text{ to } \approx 1\%!$$

\gg this is sensitive enough to probe SUSY loops, for example

\Rightarrow Higgs CP : switch to linearly polarized γ 's

e.g.,

$$T_1 = \frac{N_{H+} - N_{H-}}{N_{H+} + N_{H-}} = \frac{\langle \mathcal{J}_z \rangle + \langle \bar{\mathcal{J}}_z \rangle}{1 + \langle \mathcal{J}_z \bar{\mathcal{J}}_z \rangle} A$$

positive + negative helicity event rates
Stokes's parameters
CP Symmetry

$$A = +1 \text{ [CP even]}$$

$$-1 \text{ [CP odd]}$$

$$A \neq 1 \rightarrow \text{CP violation}$$

• e^+e^- "vs" $\gamma\gamma$: Searches for Exotic NP

(i) $e^+e^-/\gamma\gamma$ can produce anything with $Q_{em} \neq 0$

BUT e^+e^- can also make neutrals via Z^0
at tree-level **WHILE** $\gamma\gamma$ requires loops

(ii) $\sigma(\gamma\gamma \rightarrow s\bar{s}, f\bar{f}, V\bar{V}) > \sigma(e^+e^- \rightarrow s\bar{s}, f\bar{f}, V\bar{V})$

and $L_{\gamma\gamma} \approx L_{ee}$ [Figs]

BUT $\gamma\gamma$ reach is lower due to distribution(s)
cut-off

(iii) $\gamma\gamma$ probes spin-configurations not accessible
in e^+e^- , e.g., **$\gamma\gamma \rightarrow H$**

(iv) $\gamma\gamma$ isolates photonic couplings .. "cleaner"
e.g., **$\gamma\gamma \rightarrow WW$**

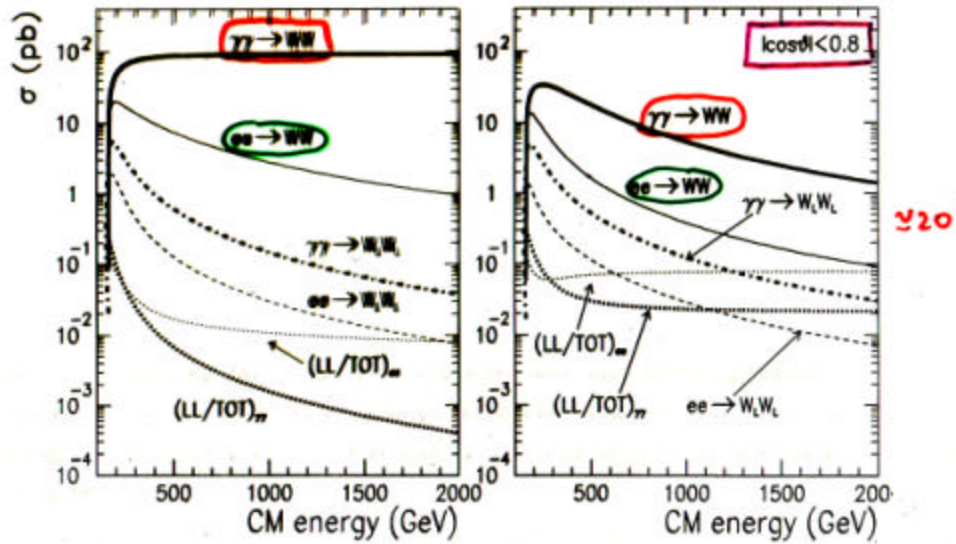
(v) $e^+e^-/\gamma\gamma$ have beam polarization(s)
 \rightarrow asymmetries $\left\{ \begin{array}{l} \text{remove backgrounds} \\ \text{NP diagnostics} \end{array} \right.$

(vi) NP analyses are not as yet evolved as in
 e^+e^-

Boillardon
 Belanger +
 Boudjema

10³

Figure 3: Comparing the total WW cross-sections and the longitudinal $W_L W_L$ in e^+e^- versus $\gamma\gamma$ as well as the ratio of longitudinal over total. For the latter, the scale can be read off on the same y axis. The second figure shows what happens when a cut on the scattering is imposed.



good news. However, one has to realize that the extraction of these longitudinals, if the new physics does not substantially increase their yield, is an incredibly tiny portion of all

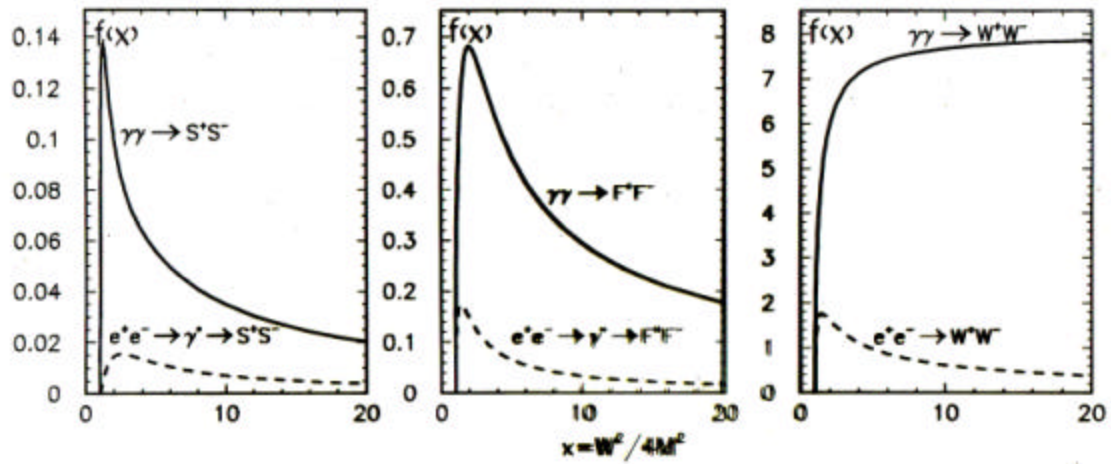
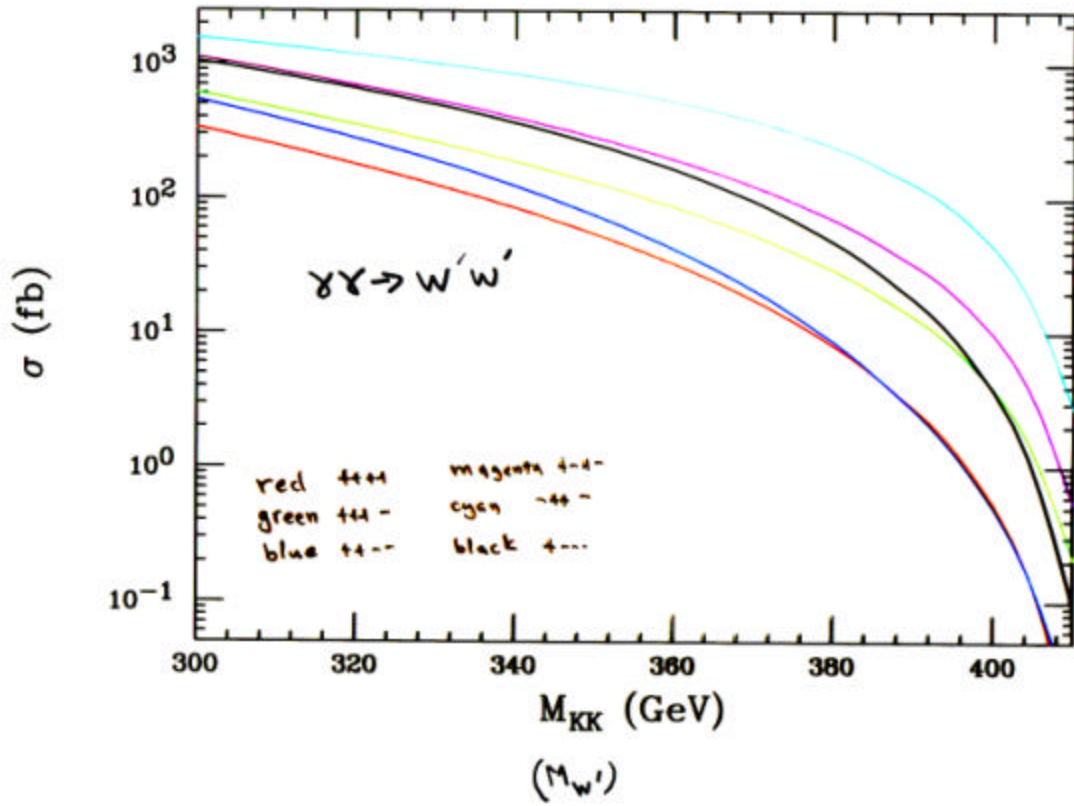
Tesla $\gamma\gamma$ 

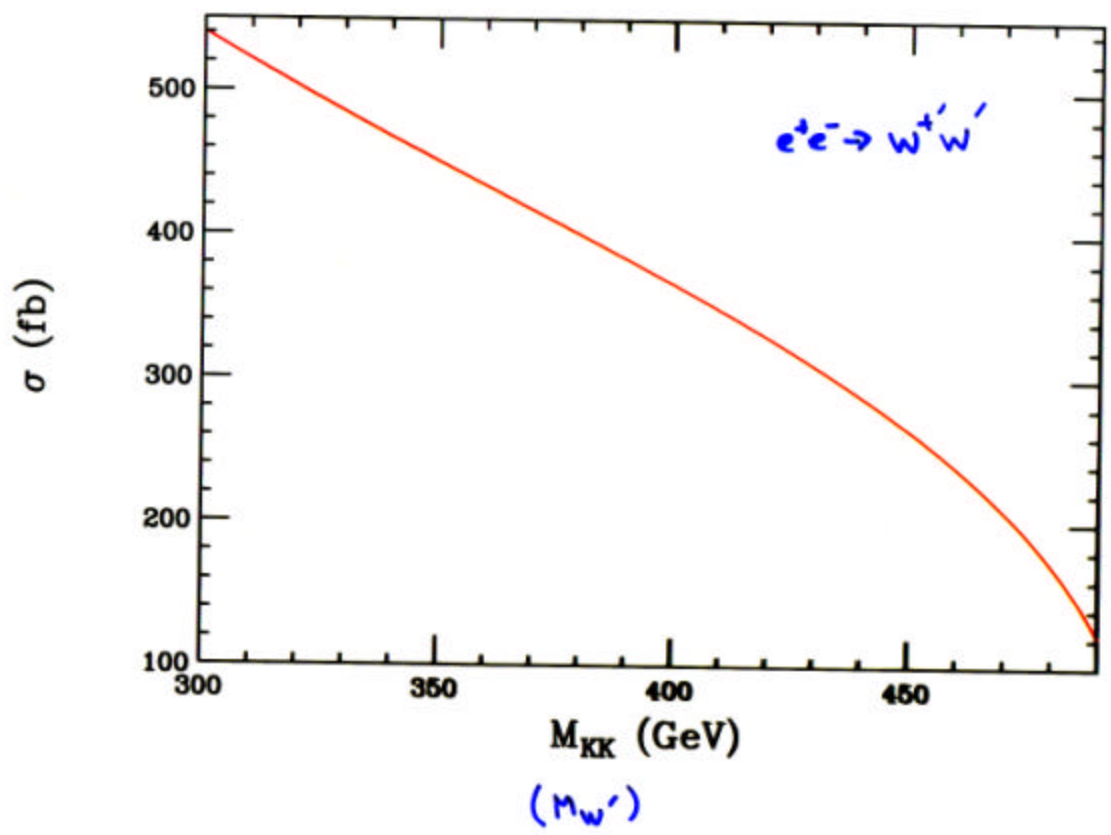
Figure 1.1.3: Comparison between cross sections for charged pair production in unpolarized e^+e^- and $\gamma\gamma$ collisions. S (scalars), F (fermions), W (W-bosons); $\sigma = (\pi\alpha^2/M^2)f(x)$, M is the particle mass, W is the invariant mass (c.m.s. energy of colliding beams), $f(x)$ are shown. Contribution of Z boson for production of S and F in e^+e^- collisions was not taken into account, it is less than 10%

$m_h = (130-250)$ GeV in $\gamma\gamma$ collisions is nevertheless 1-10 times the rate in e^+e^- collisions at 250-500 GeV

$\sqrt{s_{ee}} = 1 \text{ TeV}$



$\sqrt{s} = 1 \text{ TeV}$



• Anomalous (triple) Gauge Couplings

$$\rightarrow \lambda_{\gamma Z}, \kappa_{\gamma Z} \quad g_Z \quad \oplus \quad \cancel{SP}$$

(or some chiral Lagrangian terms)

Well studied in e^+e^- but not so in

$\gamma\gamma$ or $\gamma e \dots$ Universal issue - few

simulation studies for NP in $\gamma\gamma$ or $\gamma e \dots$

Leptoquarks / Excited fermions

Relatively easy to ID in e^+e^- using σ , $d\sigma/d\cos$

unless large form factors exist or anom. couplings

for spin-1 case or GW strength Yukawa

couplings or...

\rightarrow need $\gamma\gamma$ to disentangle things!

$\gamma\gamma \rightarrow W^+W^-$

Yehudai

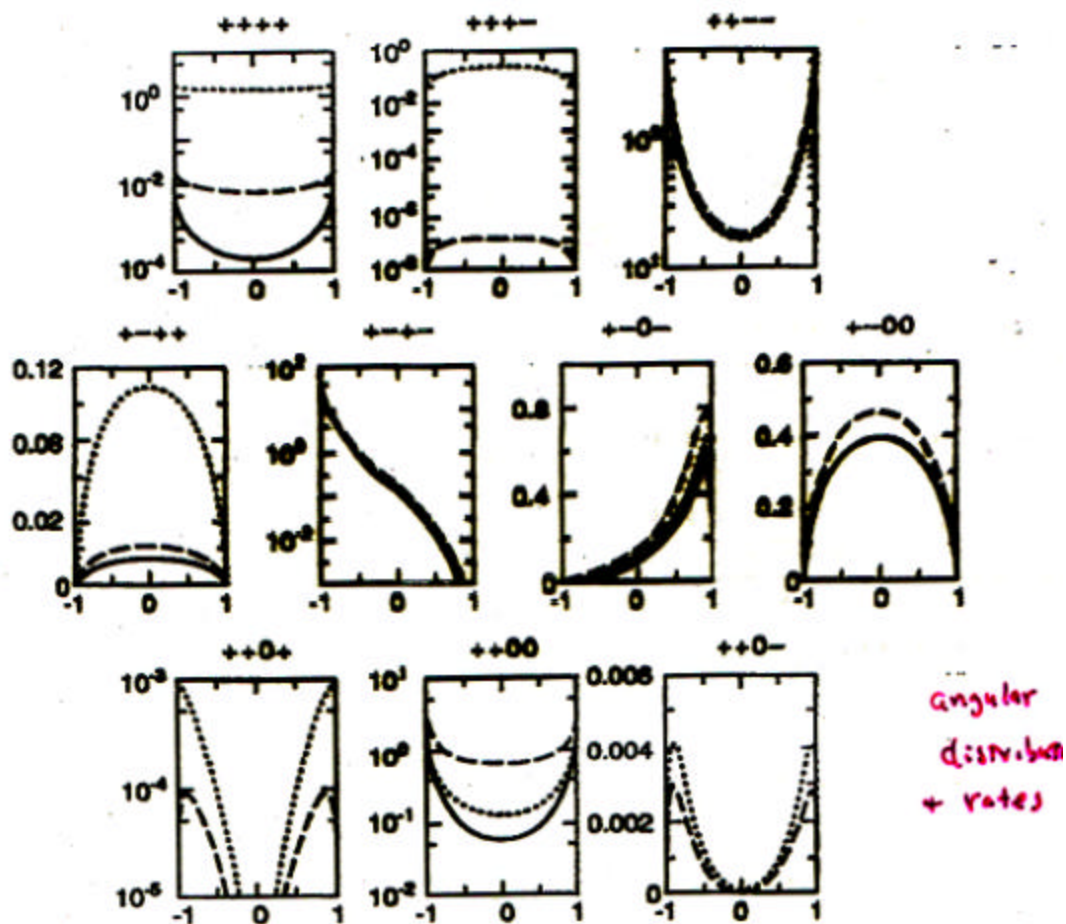
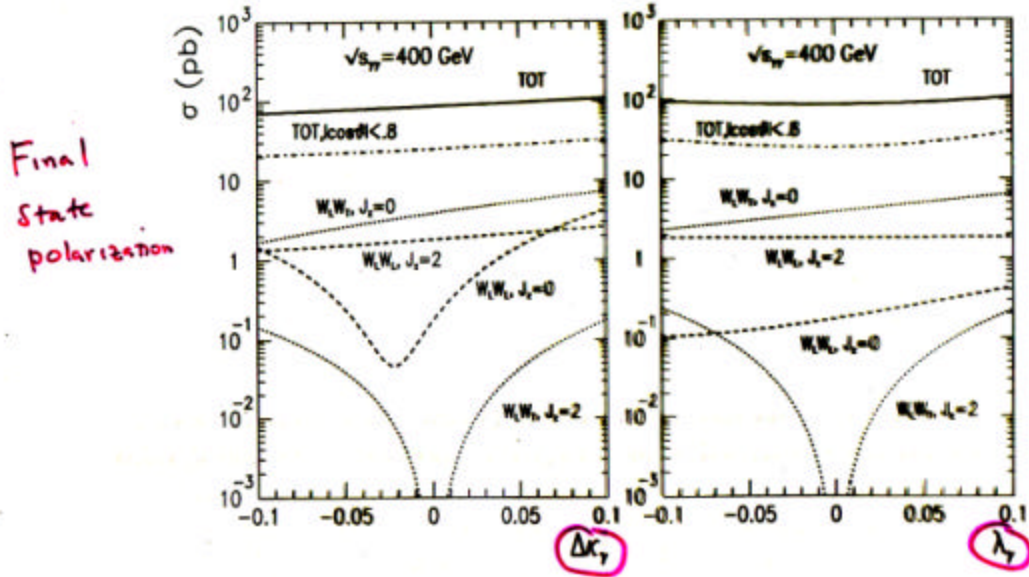


FIG. 6. Differential cross sections for producing W pairs of specific polarization with center-of-mass energy of 350 GeV as a function of $\cos\theta$. The solid lines are standard-model couplings ($\kappa=1$, $\lambda=0$). The dashed curve was calculated using $\kappa=1.1$, $\lambda=0$ while the dotted curve is for $\kappa=1$, $\lambda=-0.1$. Here and henceforth, cross sections are given in units of R .

$$\gamma\gamma \rightarrow W^+W^-$$

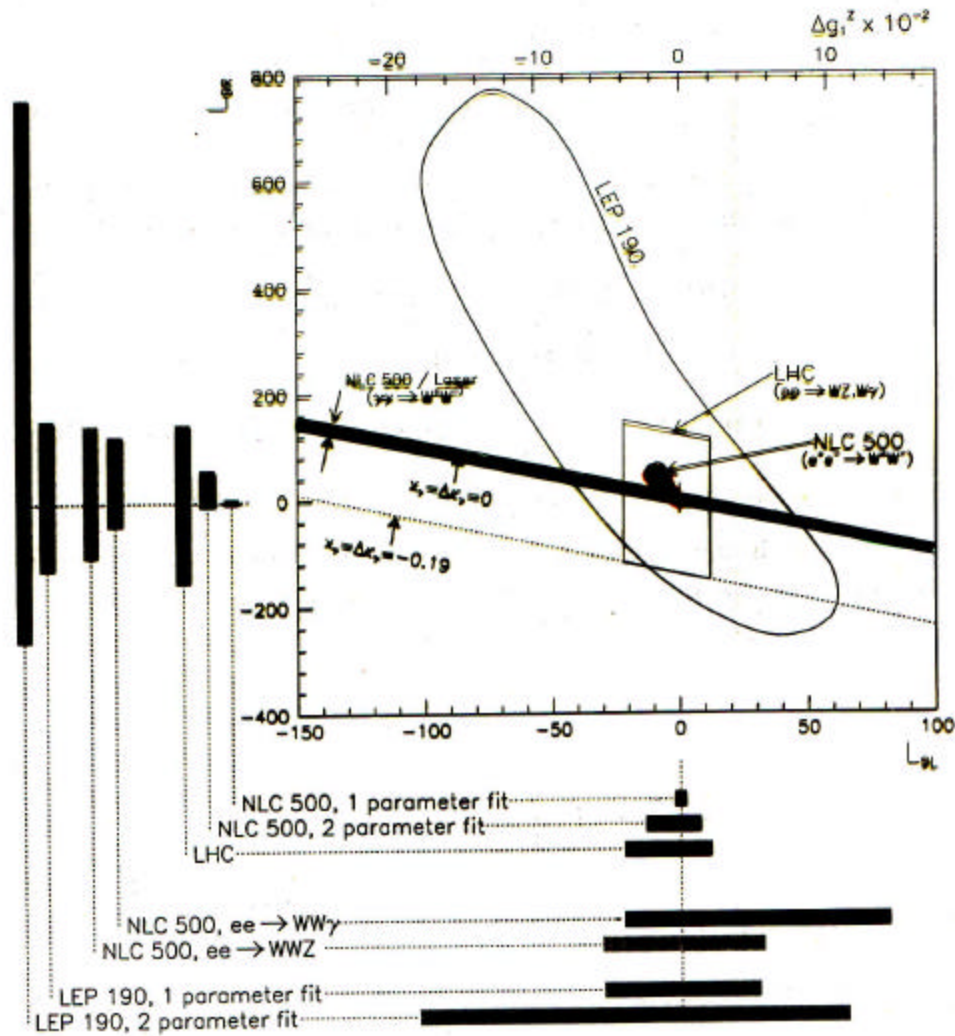
B³

Figure 8: Deviation in the various polarised cross-sections due to the anomalous couplings before folding with the spectrum. The effect of an angular cut on the total cross-section is also shown.

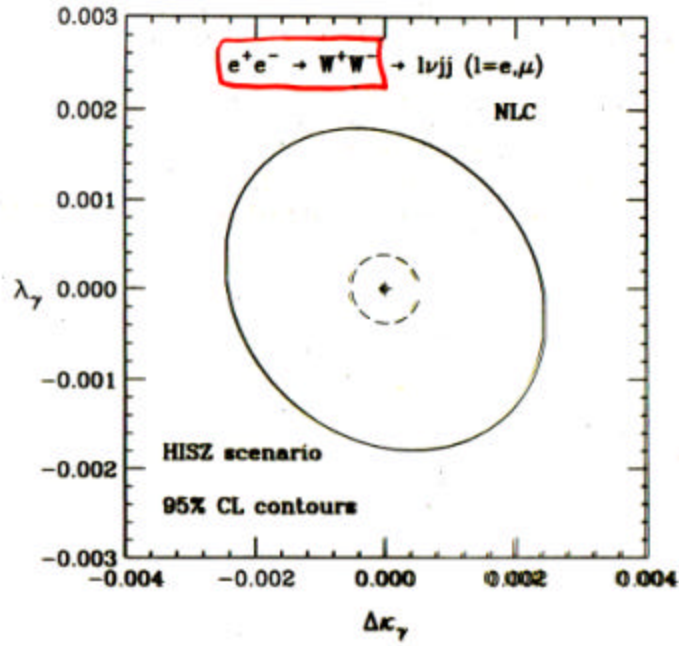


Chiral Lagrangian Parameters

Figure 10: Comparison between the expected bounds on the two-parameter space $(L_{9L}, L_{9R}) \equiv (L_W, L_B) \equiv (\Delta g_1^2, \Delta \kappa_\gamma)$ (see text for the conversions) at the NLC500, LHC and LEP2. The NLC bounds are from $e^+e^- \rightarrow W^+W^-$ [34], $W^+W^-\gamma$, W^+W^-Z [2] (for the latter these are one-parameter fits) and $\gamma\gamma \rightarrow W^+W^-$. The LHC bounds are from $pp \rightarrow WZ, W\gamma$ [43]. We also show ("bars") the limits from a single parameter fit.



Aihara et al '96



NLC
 $\Delta\kappa - \lambda \sim 10^{-3}$ level

We do a bit better now...

Figure 16: The 95% CL limit contours for $\Delta\kappa_\gamma$ and λ_γ from $e^+e^- \rightarrow W^+W^-$ at $\sqrt{s} = 500$ GeV with 80 fb^{-1} (solid line), and at $\sqrt{s} = 1.5$ TeV with 190 fb^{-1} (dashed line) for the HISZ scenario [see Eqs. (3.12)–(3.12)].

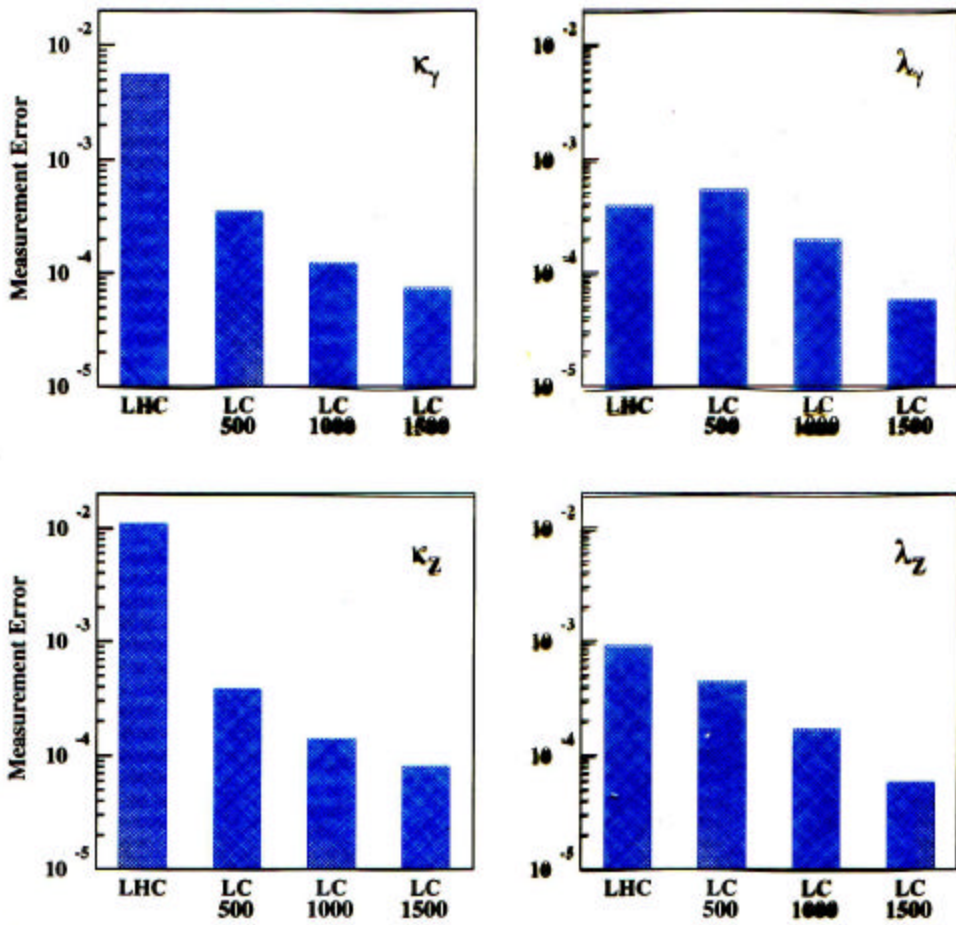
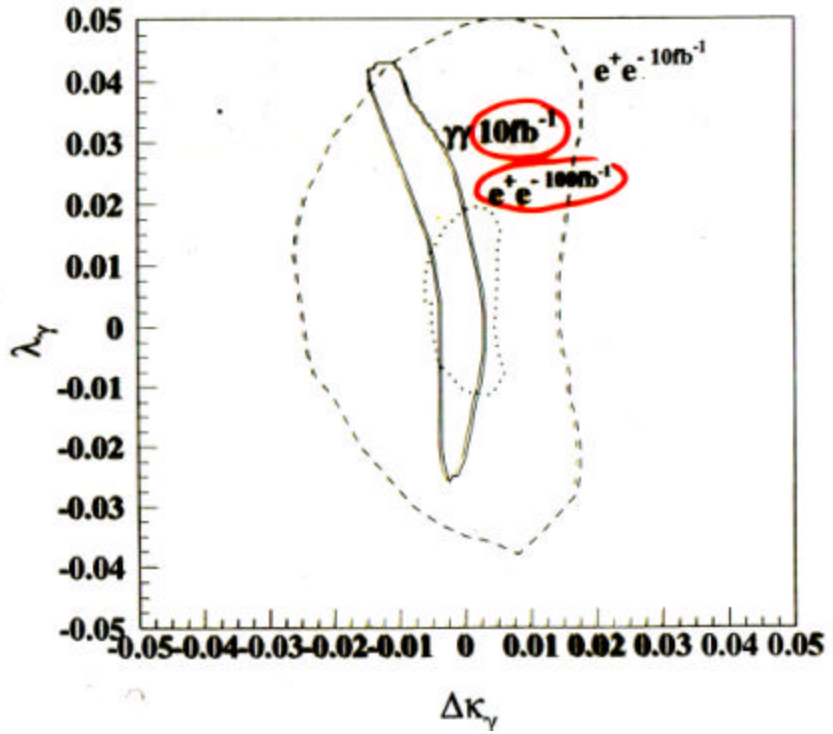


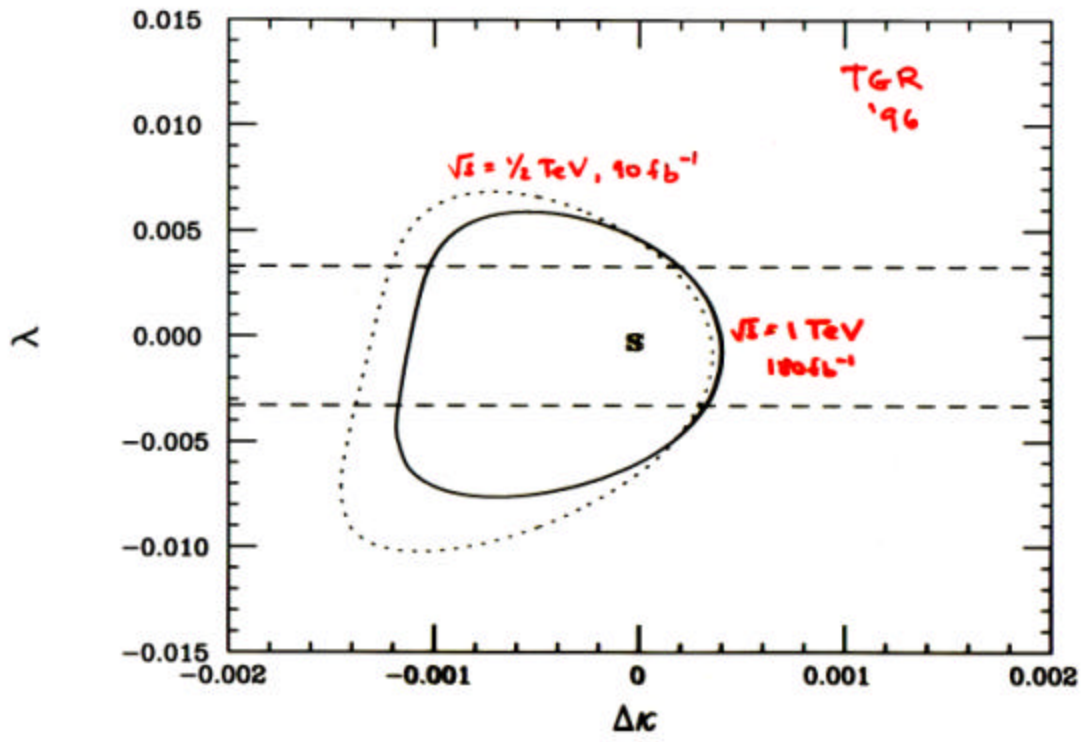
Figure 5.1: Expected measurement error for the real part of four different TGCs. The numbers below the "LC" labels refer to the center-of-mass energy of the linear collider in GeV. The luminosity of the LHC is assumed to be 300 fb^{-1} , while the luminosities of the linear colliders are assumed to be $500, 1000,$ and 1000 fb^{-1} for $\sqrt{s}=500, 1000,$ and 1500 GeV respectively.

1.2 The Physics

T. Takahashi
196



$\gamma e \rightarrow W \nu$



2.3 $\gamma\gamma \rightarrow W^+W^-$ and $\gamma e \rightarrow W\nu$

New physics beyond the SM can affect the expected values of the trilinear and quartic couplings of gauge bosons. These couplings can be studied in the reactions $\gamma e \rightarrow W\nu$ and $\gamma\gamma \rightarrow WW$, as well as in $e^+e^- \rightarrow WW$ [6]. It is noteworthy that the photon collider reactions isolate the anomalous photon couplings to the W , while $e^+e^- \rightarrow WW$ also involves anomalous Z couplings. In addition, the process $\gamma\gamma \rightarrow W^+W^-$ allows access to the quartic $\gamma\gamma W^+W^-$ coupling. The complementarity of the three reactions in determining the anomalous couplings is illustrated in Fig. 13.2, taken from [6]. Since the time of this study, it has been understood how to achieve bounds on the anomalous couplings from $e^+e^- \rightarrow WW$ that are a factor of 30 better than those shown in the figure, by taking advantage of more systematic event analysis and higher luminosities. Methods for that analysis are described in Chapter 5, Section 2. A similar improvement should be possible for the constraints from $\gamma e \rightarrow W\nu$ and $\gamma\gamma \rightarrow WW$, though the detailed study remains to be done.

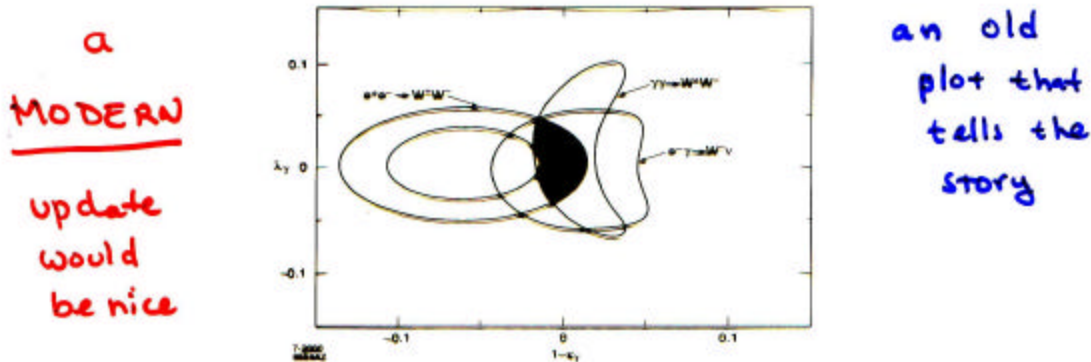


Figure 13.2: Allowed overlapping regions in the $\Delta\kappa_\gamma - \lambda_\gamma$ anomalous coupling plane, from the analysis of Choi and Schrempp [6].

1991!!

The reaction $\gamma\gamma \rightarrow W^+W^-$ is also highly sensitive to other forms of new physics such as the exchange of virtual towers of gravitons that occurs in models of millimeter-scale extra dimensions [7,8]. It has been shown that this is the most sensitive process to graviton exchange of all those so far examined. Such exchanges can lead to substantial alterations in cross sections, angular distributions, asymmetries and W polarizations. These effects make it possible to probe the associated gravitational mass scale, M_s , to values as high as $13\sqrt{s}$ for the correctly chosen set of initial laser and electron polarizations. (For comparison, the reach in e^+e^- is about $7\sqrt{s}$.) The search reach as a function of the $\gamma\gamma$ luminosity is shown in Fig. 13.3 for the various

Buchmüller, Rückl + Wyler Leptoquarks

S=0

S=1
gauge
particles
???

	Leptoquark	SU(5) Rep	Q	Coupling	B_L
Scalars					
$F = -2$	S_{1L}	5	1/3	$\lambda_L(e^+\bar{u}), \lambda_L(\bar{\nu}d)$	1/2
	S_{1R}	5	1/3	$\lambda_R(e^+\bar{u})$	1
	\tilde{S}_{1R}	45	4/3	$\lambda_R(e^+\bar{d})$	1
$F = 0$	S_{3L}	45	4/3	$-\sqrt{2}\lambda_L(e^+\bar{d})$	1
			1/3	$-\lambda_L(e^+\bar{u}), -\lambda_L(\bar{\nu}d)$	1/2
			-2/3	$\sqrt{2}\lambda_L(\bar{\nu}u)$	0
$F = 0$	R_{2L}	45	5/3	$\lambda_L(e^+u)$	1
			2/3	$\lambda_L(\bar{\nu}u)$	0
	R_{2R}	45	5/3	$\lambda_R(e^+u)$	1
			2/3	$-\lambda_R(e^+\bar{d})$	1
$F = 0$	\tilde{R}_{2L}	10/15	2/3	$\lambda_L(e^+\bar{d})$	1
			-1/3	$\lambda_L(\bar{\nu}d)$	0
Vectors					
$F = -2$	V_{2L}	24	4/3	$\lambda_L(e^+\bar{d})$	1
			1/3	$\lambda_L(\bar{\nu}d)$	0
	V_{2R}	24	4/3	$\lambda_R(e^+\bar{d})$	1
			1/3	$\lambda_R(e^+\bar{u})$	1
$F = 0$	\tilde{V}_{2L}	10/15	1/3	$\lambda_L(e^+\bar{u})$	1
			-2/3	$\lambda_L(\bar{\nu}u)$	0
	U_{1L}	10	2/3	$\lambda_L(e^+\bar{d}), \lambda_L(\bar{\nu}u)$	1/2
	U_{1R}	10	2/3	$\lambda_R(e^+\bar{d})$	1
	\tilde{U}_{1R}	75	5/3	$\lambda_R(e^+u)$	1
	J_{3L}	40	5/3	$\sqrt{2}\lambda_L(e^+u)$	1
			2/3	$-\lambda_L(e^+\bar{d}), \lambda_L(\bar{\nu}u)$	1/2
			-1/3	$\sqrt{2}\lambda_L(\bar{\nu}d)$	0

Table 1: Quantum numbers and fermionic coupling of the leptoquark states. No distinction is made between the representation and its conjugate.

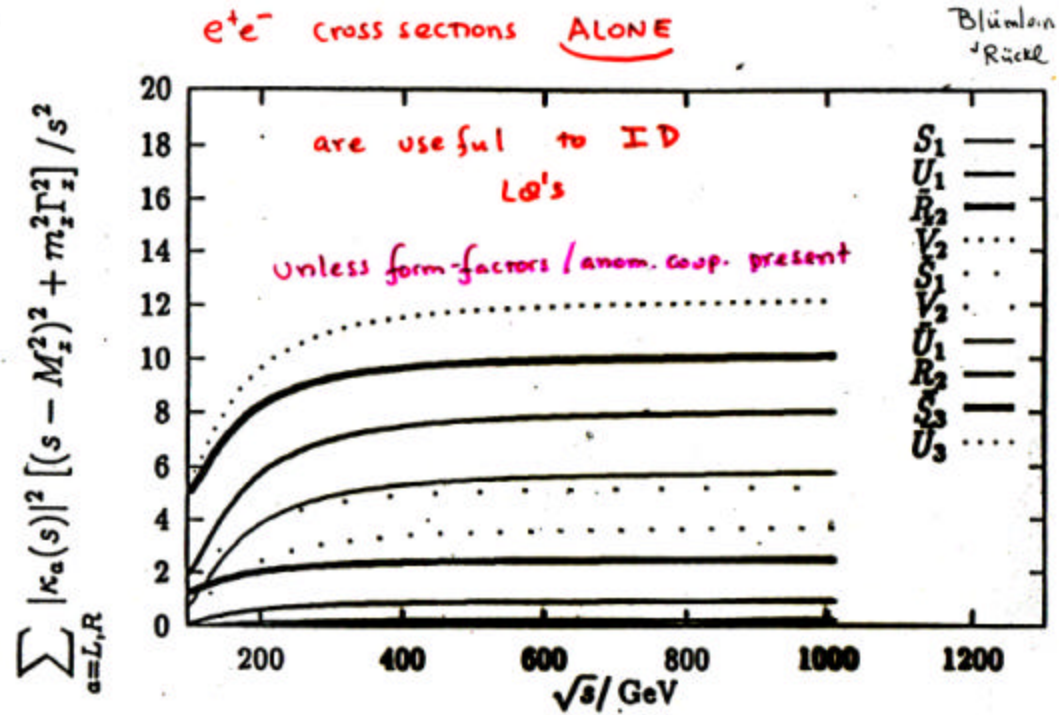


Figure 1: Energy dependence of the integrated production cross sections for scalar and vector leptoquarks. The cross sections are scaled by the factor $[(s - M_L^2)^2 + M_L^2 \Gamma_L^2] / s^2 \sigma_{\text{pt}} F_i(\beta)$ with $F_s(\beta) = 3\beta^3/8$ and $F_v(\beta) = 3\beta^3(7 - 3\beta^2)/8(1 - \beta^2)$, respectively.

Goldfrey,
London,

⋮

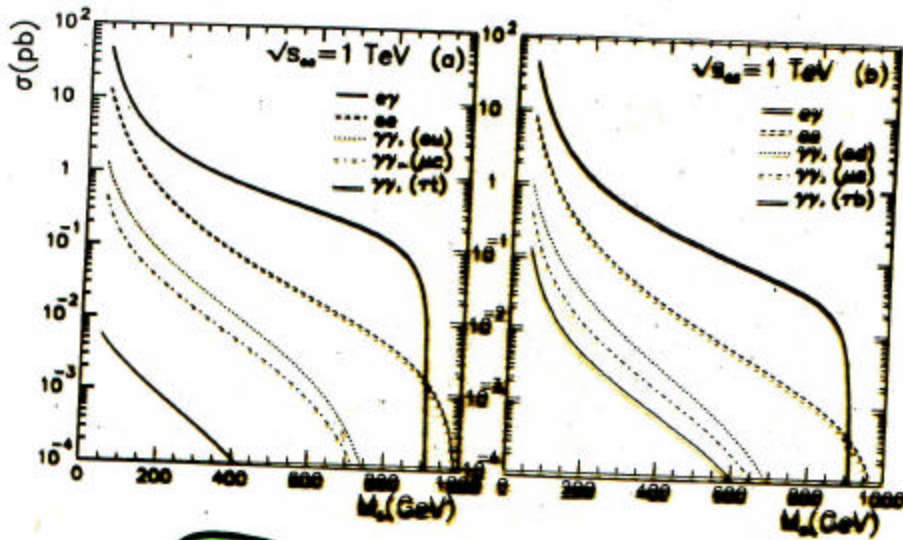


Figure 14: Single LQ production cross sections at e^+e^- , $e\gamma$ and $\gamma\gamma$ colliders for a) $Q_S = -5/3$ or $-1/3$, b) $Q_S = -4/3$ or $-2/3$.

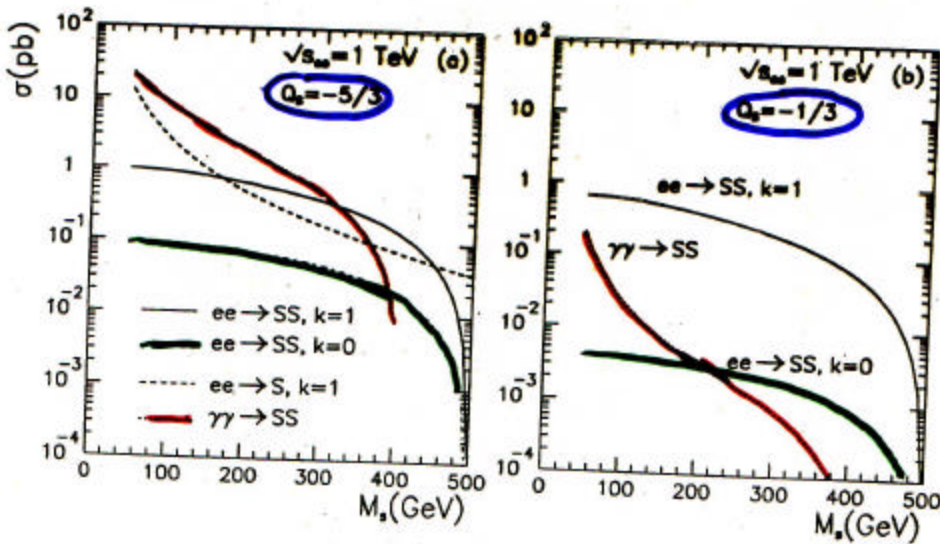
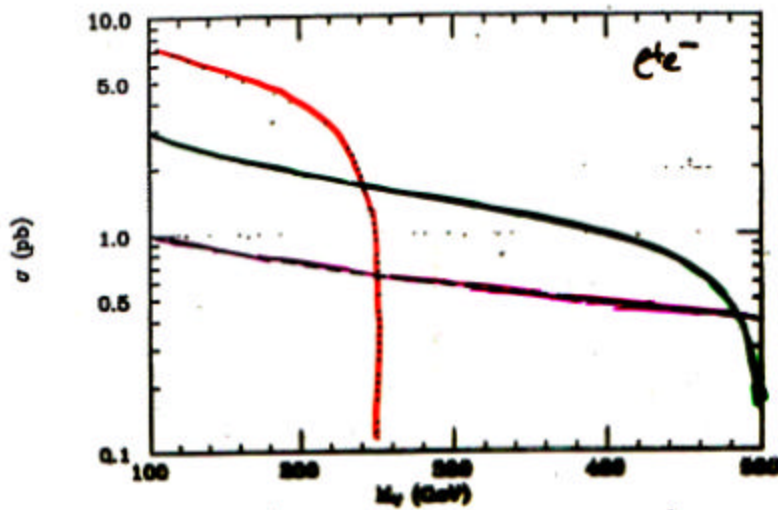


Figure 15: LQ pair-production cross sections at e^+e^- and $\gamma\gamma$ colliders.

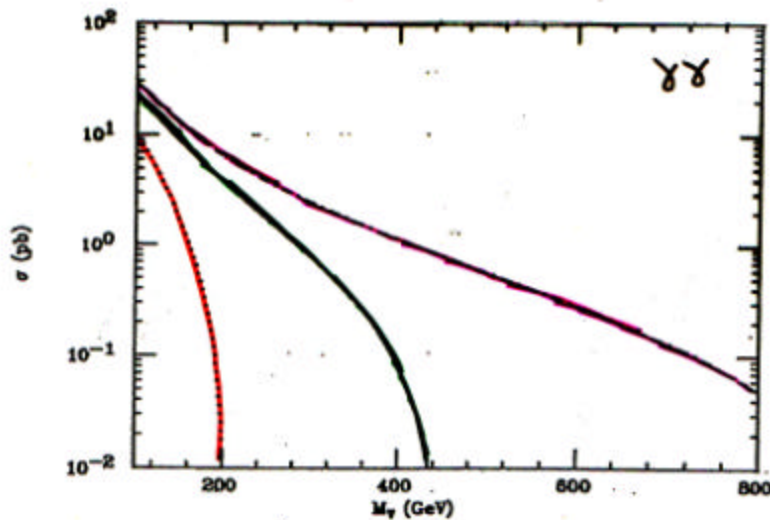


Monteloro
&
Eboli:

$e^+e^- \rightarrow V_{LQ} V_{LQ}$
vs

$\gamma\gamma \rightarrow V_{LQ} V_{LQ}$

FIG. 6. Cross section of the process $e^+e^- \rightarrow V^+V^-$ as a function of M_V for several collider energies: $\sqrt{s} = 500$ (dotted line); 1000 (solid line); 2000 (dashed line) GeV. It was assumed that $F = F_Z = \sqrt{1}$.



$Q_V = 2/3$

Spin=1
LQ

Gauge Bosons

FIG. 8. Same as in Fig. 7, but with the γ 's produced by laser backscattering.

Excited fermions

Boujemra
Djouadi

444

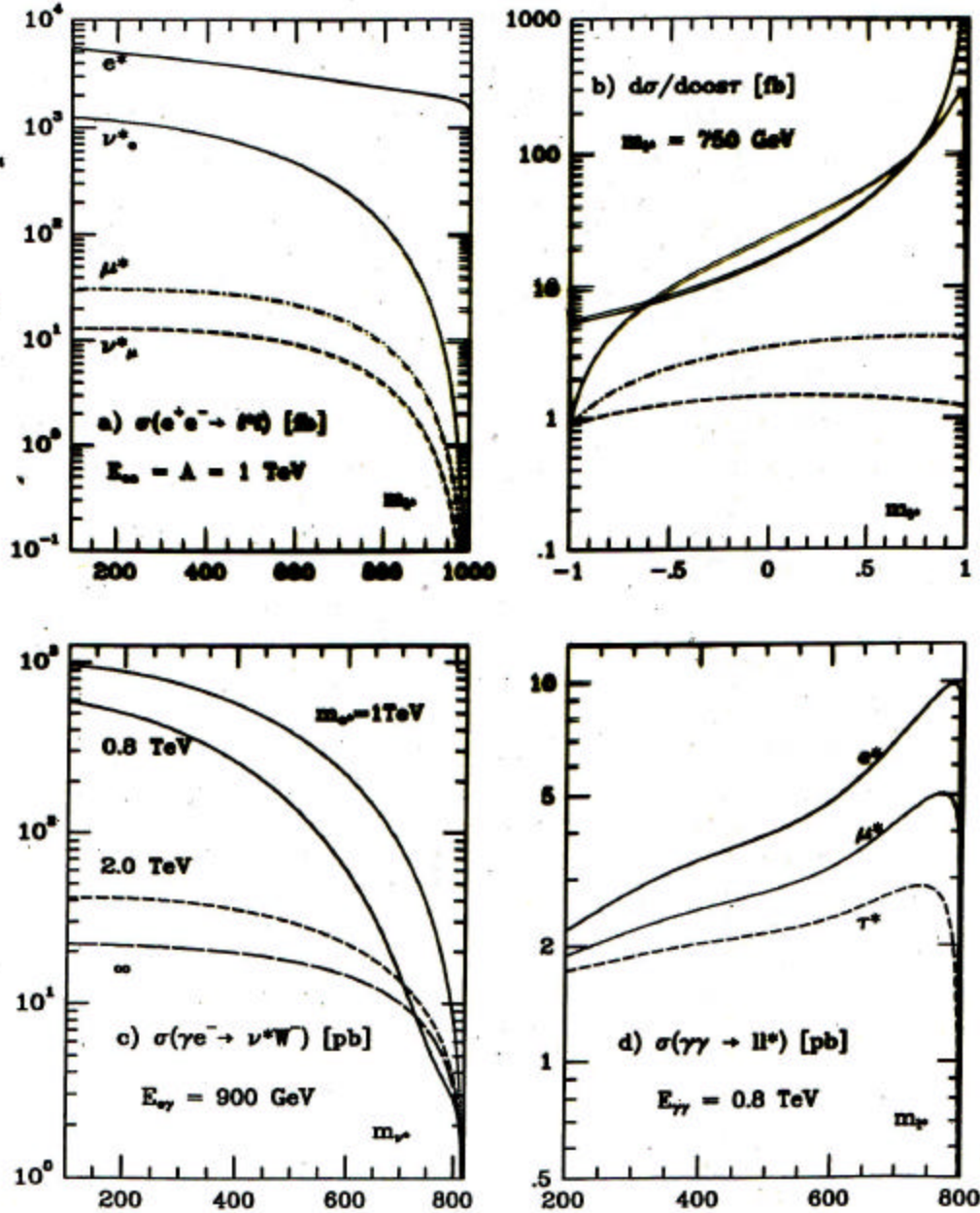


Figure 10: Cross sections for the single production of excited fermions in e^+e^- collisions with $\sqrt{s} = 1$ TeV (a,b), of excited neutrinos in $e\gamma$ collisions (c) and of excited charged fermions in $\gamma\gamma$ collisions (d).

Single Top Production

$$\gamma e_L \rightarrow \nu \bar{t} b$$

- Directly proportional to g_{Wtb}
- Most general interaction:

$$\frac{g}{\sqrt{2}} \left[W_{\mu}^{-} \bar{b} (\gamma_{\mu} f_{1L} P_{-} + \gamma_{\mu} f_{1R} P_{+}) t \right. \\ \left. - \frac{1}{2M_W} W_{\mu\nu} \bar{b} \sigma^{\mu\nu} (f_{2R} P_{-} + f_{2L} P_{+}) t \right]$$

- Expected limits on f_2^L couplings:

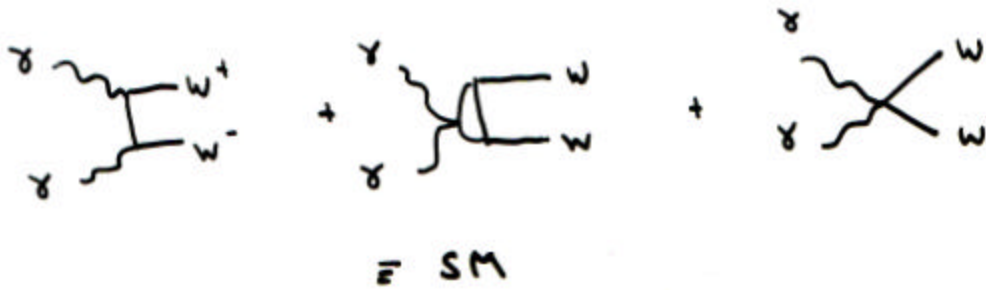
<i>Tevatron</i> ($\Delta_{sys.} \approx 10\%$)	$-0.18 \div +0.55$
<i>LHC</i> ($\Delta_{sys.} \approx 5\%$)	$-0.052 \div +0.097$
γe ($\sqrt{s_{e^+e^-}} = 0.5 \text{ TeV}$)	$-0.1 \div +0.1$
γe ($\sqrt{s_{e^+e^-}} = 2.0 \text{ TeV}$)	$-0.008 \div +0.035$

(Boos, hep-ph/0103090)

- Similar results for other couplings
- Best limits are from $e\gamma$

Extra dimensions

e.g. : in $\gamma\gamma \rightarrow W^+W^-$



distortions of
SM σ 's \oplus
New physics
NOT in SM

But not just $W^+W^-^{(*)}$

ALL final states : $t\bar{t}^{(*)} / b\bar{b}^{(*)} / \gamma\gamma^{(*)} / \tau\tau^{(*)} / HH^{(*)} \dots$

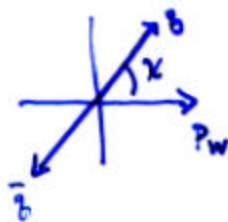
↑
Hooman
Davoudiasl

* TGR

$$\boxed{\gamma\gamma \rightarrow W^+W^-}$$

- Huge cross section in SM $\sim 100 \underline{\underline{\text{pb}}}$
 [$\gamma\gamma \rightarrow q\bar{q}$ much smaller]
- Simple SM amplitude, tree-level no SUSY contributions
- No K-K W', γ', Z' contributions
- More observables!

\Rightarrow W helicity can be reconstructed in W r. frame



$$\sim (1 \pm \cos^2 \chi) \begin{cases} + = T \\ - = L \end{cases}$$

\therefore TT, TL, LL fractions gotten via correlations

\Rightarrow M_{WW} can be constructed in 4jet + 2jet + $\ell\bar{\ell}$ cases
 "without" backgrounds

[Polarization Asymmetries] " $\gamma\gamma \uparrow\uparrow$ vs. $\gamma\gamma \uparrow\downarrow$ "

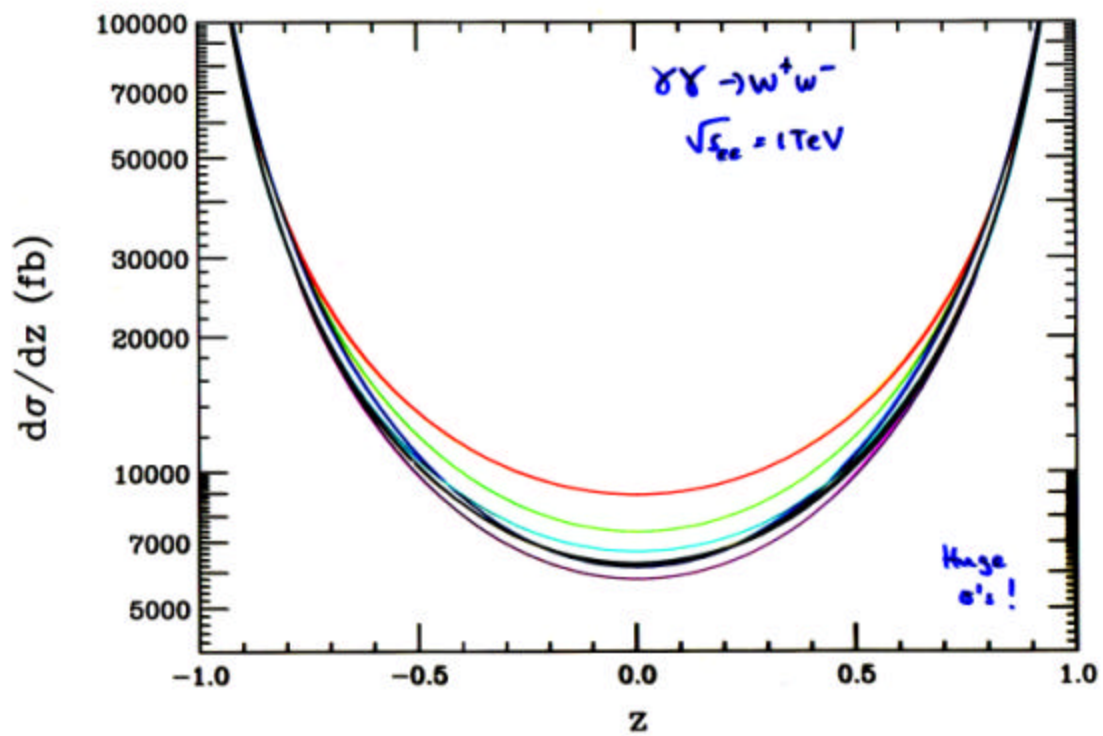
- angular dependencies
- M_{ww} "

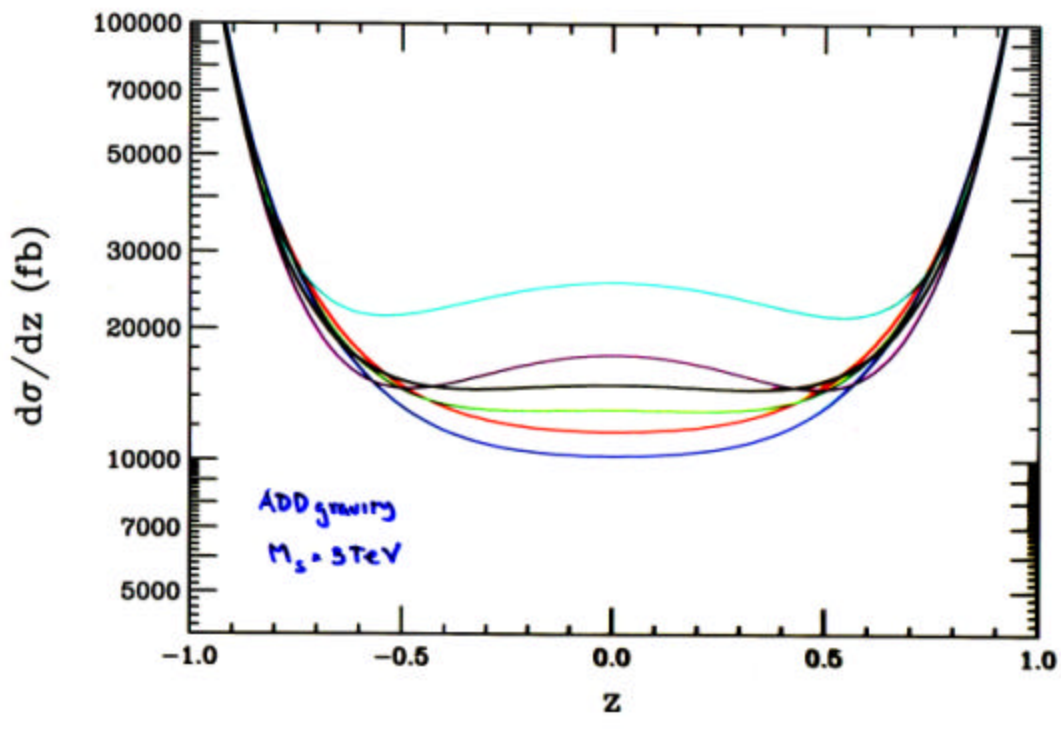
\Rightarrow Drell-Hearn - Gerasimov
Sum Rule

- asymmetry zero in
 $A(M_{ww})$ must be present

\Rightarrow NOT included in fits

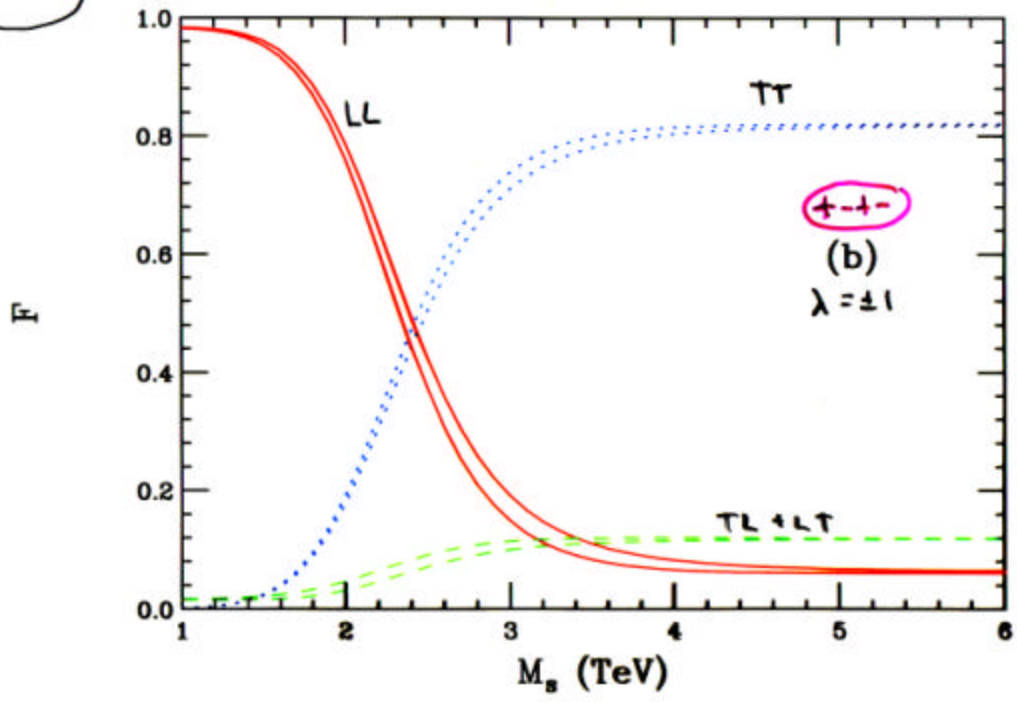
{ Flip laser 2 / electron 2 polarization }



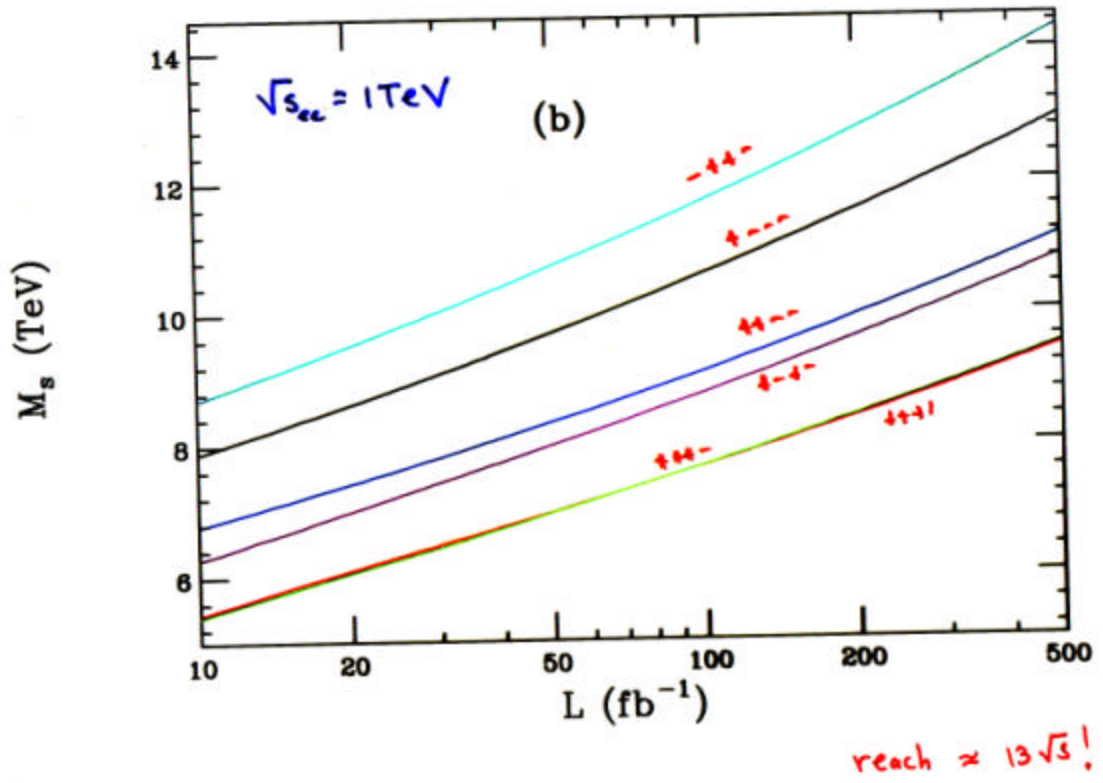


Final
State
Helicity

$$\gamma\gamma \rightarrow W^+W^- \quad \sqrt{s} = 1 \text{ TeV}$$



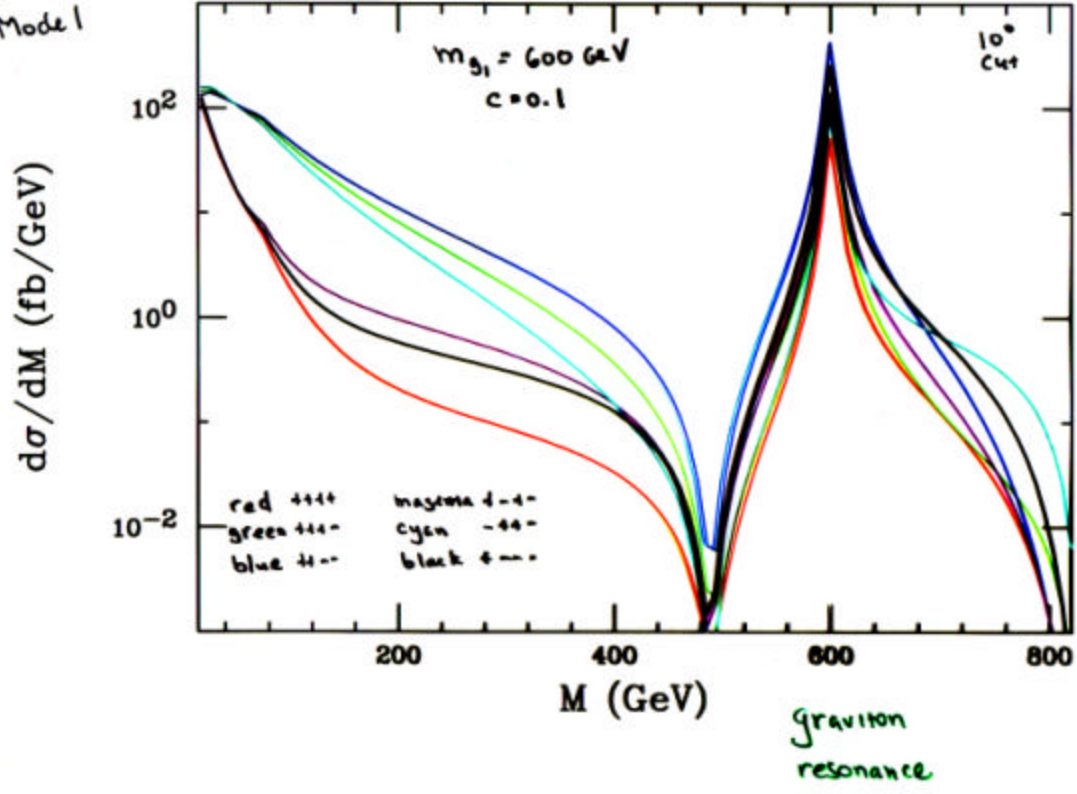
$\gamma\gamma \rightarrow W^+W^-$ search reach



Randall
Sundrum
Model

$\gamma\gamma \rightarrow b\bar{b}$

$\sqrt{s} = 1 \text{ TeV}$



Conclusions :

- $\gamma\gamma$ and e^+e^- play complementary roles in discovering / searching / examining NP
- In some cases, like $\gamma\gamma \rightarrow WW$ in ADD $\gamma\gamma$ is by far the most sensitive process
- $\gamma\gamma$ physics still needs more MC detailed study w/ detector 'issues'
- $\gamma\gamma$ would be a beneficial part of any future linear collider program
- For more NP come to the session
!!!